

Article

Hydrogen Sensing Properties of Co-Doped ZnO Nanoparticles

Fatemeh Moosavi ¹, Mohammad Ebrahim Bahrololoom ¹, Ramin Kamjou ², Ali Mirzaei ³, Salvatore Gianluca Leonardi ⁴  and Giovanni Neri ^{4,*} 

¹ Department of Materials Science and Engineering, Shiraz University, Shiraz 71964-84334, Iran; Fateme.moosavi68@gmail.com (F.M.); bahrolom@shirazu.ac.ir (M.E.B.)

² Young Researchers and Elite Club, Islamic Azad University, Shiraz Branch, Sadra city, Shiraz 74731-71987, Iran; rkamjou@gmail.com

³ Department of Materials Science and Engineering, Shiraz University of Technology, Shiraz 71557-13876, Iran; alisonmirzaee@yahoo.com

⁴ Department of Engineering, University of Messina, Contrada di Dio, I-98166 Messina, Italy; Leonardis@unime.it

* Correspondence: gneri@unime.it

Received: 28 October 2018; Accepted: 3 December 2018; Published: 5 December 2018



Abstract: In this study, the gas sensing properties of Co-doped ZnO nanoparticles (Co-ZnO NPs) synthesized via a simple sol-gel method are reported. The microstructure and morphology of the synthesized Co-ZnO NPs were characterized by X-ray diffraction (XRD) and transmission electron microscopy (TEM), respectively. Co-ZnO NPs were then used for developing a conductometric gas sensor for the detection, at mild temperature, of low concentration of hydrogen (H₂) in air. To evaluate the selectivity of the sensor, the sensing behavior toward some VOCs such as ethanol and acetone, which represent the most important interferents for breath hydrogen analysis, was also investigated in detail. Results reported demonstrated better selectivity toward hydrogen of the Co-ZnO NPs sensor when compared to pure ZnO. The main factors contributing to this behavior, i.e., the transition from *n*-type behavior of pristine ZnO to *p*-type behavior upon Co-doping, the modification of oxygen vacancies and acid-base characteristics have been considered. Hence, this study highlights the importance of Co doping of ZnO to realize a high performance breath hydrogen sensor.

Keywords: Co-doped ZnO; nanoparticle; sol-gel; hydrogen; ethanol; gas sensor; sensing mechanism

1. Introduction

ZnO has been one of the most investigated material for gas sensing by using conductometric sensors, i.e., devices whose response is related to the resistance variation of the sensitive element upon exposure to target gases [1]. In the pristine form, ZnO is an *n*-type semiconducting metal oxide with a wide direct band gap (~3.3 eV), high exciton binding energy (60 meV), excellent chemical and thermal stability, and a low price [2,3]. Nanosized ZnO due to fascinating properties imprinted by the small dimension is used in the transparent electrodes [4], solar cells [5], transducers [6], optoelectronic devices [7], UV sensors [8], and gas sensors [9,10]. Regarding gas sensing application, nanostructured ZnO materials have been reported for detection of both oxidative and reducing gases such as various VOCs [11–15], LPG [2], acetylene [16], NO₂ [17], ammonia [18], and H₂ [19] with good performance. ZnO-based sensors are often preferred to other metal oxide-based conductive sensors to detect gaseous species due to their particular features such as high sensitivity, ease of fabrication, and very low cost [20].

ZnO has been largely investigated for H₂ sensing [21–24]. Sensing properties toward this gas are particularly remarkable when ZnO is in a nanostructured form [25]. However, doping ZnO with

noble metals such as Pd is a somewhat required additional step to obtain the desired high sensitivity for advanced applications. For example, Wang et al. [26] employed ZnO nanorods coated with Pd to detect H₂ down to 10 ppm with a relative response of 2.6% at 10 ppm and a recovery time of less than 20 s at 25 °C.

On the other hand, noble metals are expensive. Therefore, we decided to focus our attention on developing high performance doped-ZnO sensors for hydrogen by using cheaper additives/modifiers. In this case, we report the research activity made to investigate the hydrogen sensing properties of Co-doped ZnO sensor. There are few studies reporting on the addition Co on ZnO and leading to the formation of Co₃O₄/ZnO heterojunctions with *p*-type behavior [27]. Co-doped ZnO nanocomposites show good sensing properties toward H₂ monitoring at very low concentration, which is of utmost importance for detecting this gas in the human breath [28]. Hydrogen found in the breath of humans can be an indicator of some diseases like neonatal necrotizing enterocolitis, lactose intolerance, fructose malabsorption, and diabetic gastroparesis. Accordingly, high performance hydrogen sensors are of utmost importance and are highly demanding in the biomedical field.

However, one of the biggest drawbacks of metal oxide conductometric hydrogen sensors is the cross-sensitivity to other gases present in the breath, especially acetone (C₃H₆O) and ethanol (C₂H₅OH). These two volatile organic compounds (VOCs) are present in the breath of humans and their concentrations varies as a consequence of different factors. For instance, while the concentration of ethanol in the breath of healthy people is almost negligible, its concentration reach high levels for many hours after drinking alcoholic beverages in excess [29,30]. In addition, acetone is present in higher concentrations in the breath under particular circumstances [31]. People with cases of diabetes that are not well controlled and suffering of ketoacidosis show higher levels of breath acetone compared to healthy people.

In this study, we synthesized pristine and Co-doped ZnO NPs by a facile and low temperature sol-gel method and investigated their electrical and sensing characteristics towards the monitoring of low hydrogen concentration. In particular, we focused our attention on the role of Co dopant in modifying the sensing characteristics of pristine ZnO for H₂ monitoring at low concentration and selectivity against ethanol.

2. Materials and Methods

2.1. Synthesis of Co-Doped ZnO

In order to synthesize Co-doped ZnO NPs, zinc acetate dihydrate (Zn(CH₃COO)₂·2H₂O), cobalt acetate tetrahydrate (Co(CH₃COO)₂·4H₂O), isopropanol (CH₃C₂H₅OH), and monoethanolamine (C₂H₇NO) were used. All chemicals used in the experiment were of analytical grades. Doped ZnO NPs were synthesized by the following procedure. First, 0.917 g (0.005 mol) (Zn(CH₃COO)₂·2H₂O) was dissolved in 10 mL isopropanol. Then 0.060 g (0.001 mol) monoethanolamin was added to the Zn²⁺ solution as a stabilizer. Subsequently, 0.249 g (0.001 mol) (Co(CH₃COO)₂·4H₂O) was added to the above solution and the obtained solution was stirred at 70 °C for 1 h to accelerate the hydrolysis reactions. The final solution was clear in color and homogeneous. After three weeks kept at room temperature, the solution was changed to a highly viscous gel. Lastly, the obtained gel was calcined at 400 °C for 1 h in a muffle furnace. For synthesis of pristine ZnO NPs, the procedure was the same. However, in this case, the cobalt precursor was not added to the prepared solution.

2.2. Characterization

Phase and crystallinity of synthesized powders were analyzed by X-ray diffraction. XRD data were collected by a Bruker D8 Advance Diffractometer (Bruker AXS, Karlsruhe, Germany) using the CuK_{α1} wavelength of 1.5405 Å. Morphological analysis was carried out by using transmission electron microscopy (TEM-Philips CM 200, Philips, Eindhoven, Netherlands).

2.3. Gas Sensing Measurements

Gas sensors were fabricated as follows: first, synthesized nano-powders were mixed with distilled water and deposited on cleaned Al_2O_3 sensor substrates by a drop coating method. The size of the sensor substrate platform was $6\text{ mm} \times 3\text{ mm}$ and comprised a pair of interdigitated Pt electrodes on the front side and a resistive heater on its backside. The sensing area where the ZnO or Co-doped ZnO sensing material had to be deposited is $2\text{ mm} \times 2\text{ mm}$. Before sensing tests, the sensor was conditioned in air for 2 h at $300\text{ }^\circ\text{C}$. Hydrogen sensing tests were performed by injecting pulses of the target gas from certified bottles and measuring the change in resistance. The sensors were tested at different temperatures under a synthetic dry air stream of 100 sccm as carrier gas. By collecting the resistance data in the four-point mode, the gas response, S , was defined as $S = R_0/R$ (for pristine sensor) or $S = R/R_0$ (for Co-doped gas sensor) where R_0 is the baseline resistance in air and R is the electrical resistance of the sensor in the presence of hydrogen or other gases tested, respectively. The response time is defined as the time required for a sensor to reach 90% of its final value after introducing the gas pulse and the recovery time was defined as the time required for the sensor to reach 90% of its original baseline signal after returning to air flow.

3. Results

3.1. Morphological and Microstructural Characterization

The TEM micrograph of Co-doped ZnO sensor is shown in Figure 1. As can be seen, it consists of ZnO NPs with a hexagonal shape and with an approximate size of 25 nm.

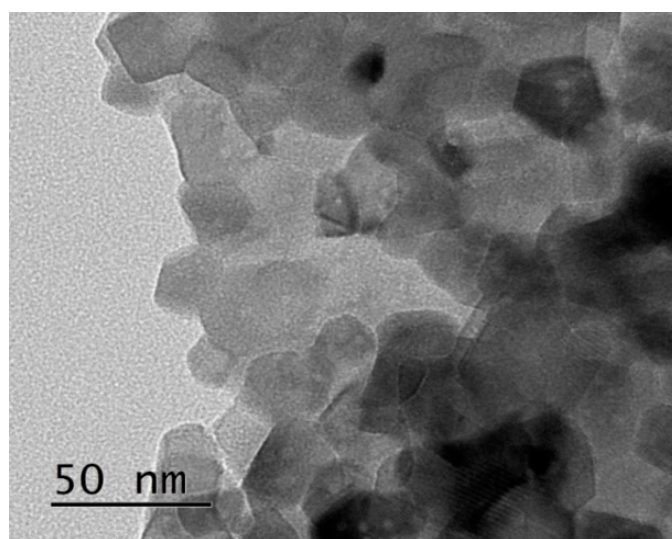


Figure 1. TEM micrograph of Co-doped ZnO NPs.

Figure 2 shows the XRD pattern of pristine ZnO and Co-doped ZnO NPs. The XRD pattern of pristine ZnO shows diffraction peaks related to the formation of ZnO with the hexagonal wurtzite structure while no other peaks due to the presence of impurities were observed. In the XRD pattern of Co-doped ZnO NPs, peaks related to both crystalline ZnO and Co_3O_4 phases can be observed. The co-dopant can mainly be sorted into two categories: (i) in the crystal lattice substituting the original atom and (ii) forming other phases besides the original one [25]. From the XRD data reported in this study, it appears that Co_3O_4 has been formed as a separate phase. However, it cannot be excluded that a part of Co replaces Zn in the ZnO lattice. This could occur with little or without change of the ZnO wurtzite structure due to the small difference between the ionic radius of the Zn (0.740 \AA) and Co (0.745 \AA).

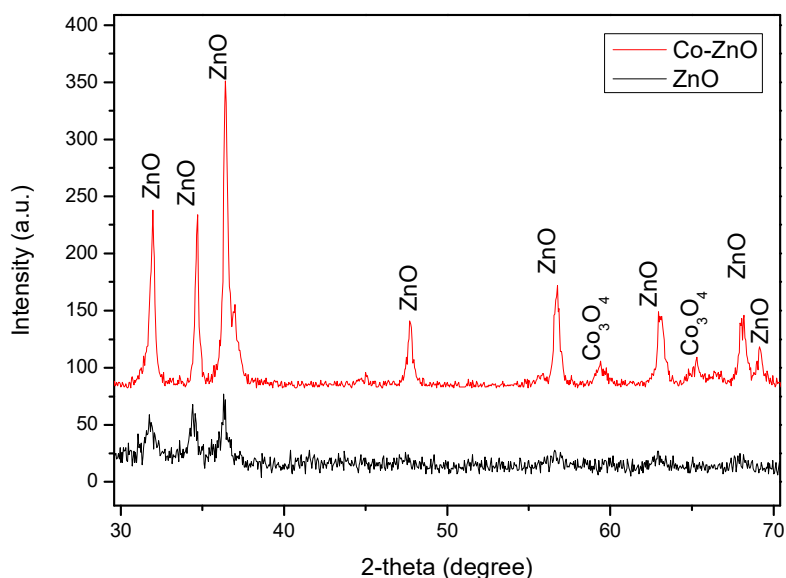


Figure 2. XRD patterns of pristine ZnO and Co-doped ZnO NPs.

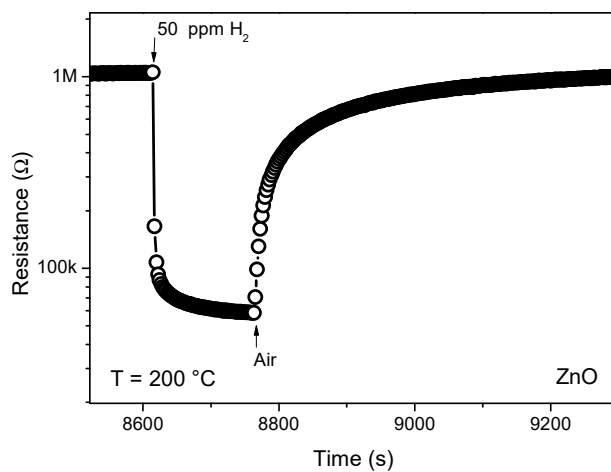
3.2. Sensing Tests

First, the gas sensing properties of pristine ZnO and Co-doped ZnO sensors were compared. It is well known that the performances of the semiconductor gas sensors are greatly influenced by the working temperature because gas adsorption, reaction, and desorption are temperature-dependency phenomena [11]. Preliminary tests (not shown) indicated that the fabricated ZnO and Co-doped ZnO sensors shows best performances in the temperature range between 150 °C to 250 °C.

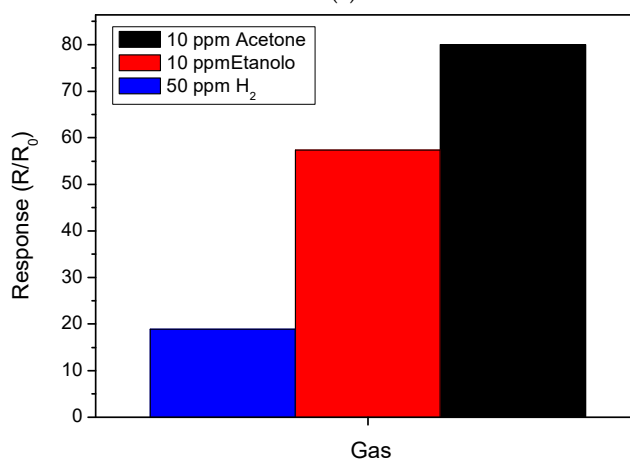
Thus, to compare the sensing performances of these sensors, the operating temperature was set at 200 °C. Figure 3a reports the transient response to 50 ppm of H₂ on ZnO sensor. In the presence of hydrogen, the resistance show a fast decrease. The response is very high ($S = 18$). However, one limitation of this ZnO sensor is the cross-sensitivity of other gases present in the breath and in specifically acetone and ethanol. This is well evident in Figure 3b where the response of the pristine ZnO sensor to hydrogen is compared with the higher response observed when exposed to the previously mentioned VOCs.

The sensing behavior of Co-doped ZnO sensor in the same conditions have been evaluated and reported in Figure 4a,b. Using this comparison, some findings appear to be very clear. First, a pristine ZnO gas sensor shows *n*-type semiconducting behavior while the Co-doped gas sensor shows a clear *p*-type behavior, which indicates a change of the semiconducting behavior upon Co-doping [32]. Second, even if the pristine ZnO sensor is more sensitive than the Co-doped ZnO gas sensor, its selectivity to hydrogen is poorer. Furthermore, the Co-doped ZnO sensor shows a faster dynamics response compared to a pristine ZnO sensor. The response and recovery time of the Co-doped ZnO based sensor are 20 s and 150 s, respectively. The recovery time is much shorter than that observed with the pristine ZnO sensor (>200 s). This suggests that the desorption stage represents the rate-determining step for the overall process.

Figure 5a,b show dynamic resistance curves of pristine ZnO and Co-doped ZnO NPs, respectively, registered at 200 °C toward a pulse of 10 ppm ethanol. As previously mentioned, the Co-doped ZnO sensor shows a lower response to ethanol in comparison to the pristine ZnO sensor, which is advantageous because it means that this gaseous species present low interference for the determination of breath hydrogen. The response time is faster for the Co-doped ZnO sensor (less than 50 s) when compared to the pristine ZnO-based sensor (around 200 s). Furthermore, a longer recovery time has been recorded for the pristine ZnO-based sensor (around 750 s) when compared to the Co-doped one (less than 200 s).

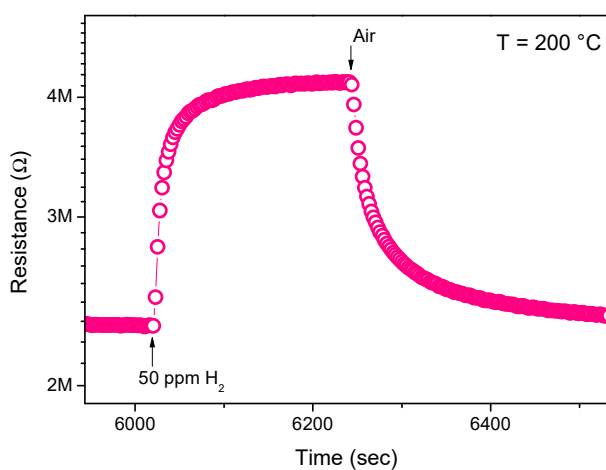


(a)



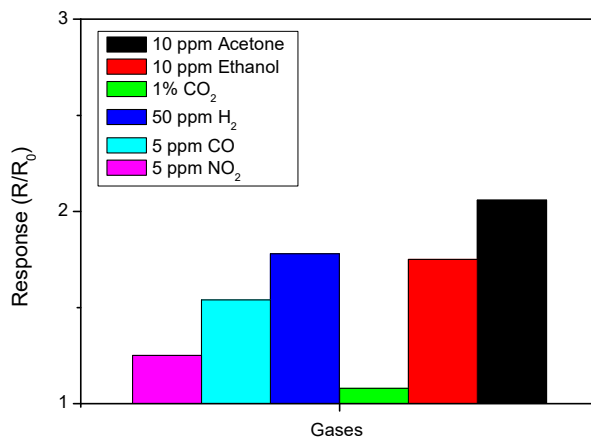
(b)

Figure 3. (a) Transient response to 50 ppm of H₂ of the ZnO sensor. (b) Comparison of the response of the ZnO sensor to H₂, acetone, and ethanol.



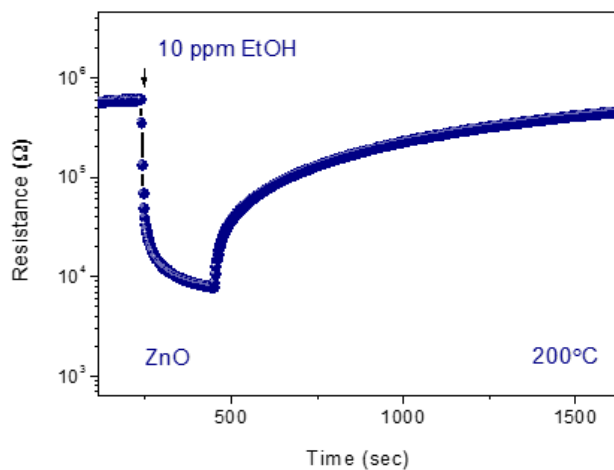
(a)

Figure 4. Cont.

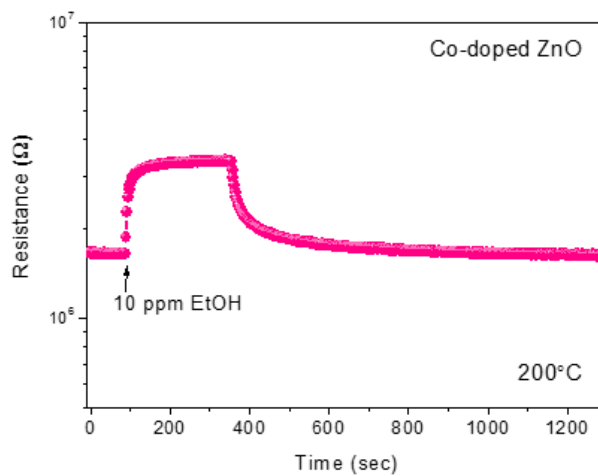


(b)

Figure 4. (a) Transient response to 50 ppm of H₂ of Co-doped ZnO sensor. (b) Comparison of the response of Co-doped ZnO sensor to H₂, acetone, ethanol, and other environmental interferent gases.



(a)

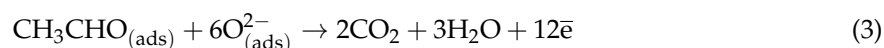
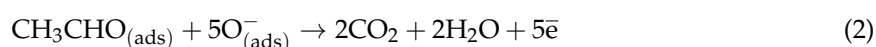
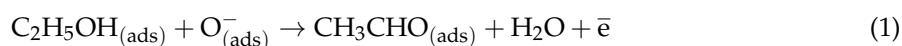


(b)

Figure 5. Response to 10 ppm of ethanol gas at different temperatures for (a) ZnO and (b) a Co-doped ZnO gas sensor.

A possible reason behind the decrease of response of the Co-doped sensor toward ethanol is the decrease of oxygen vacancies in ZnO due to Co-doping. In fact, *n*-type behavior in pristine ZnO suggests the presence of oxygen vacancies, which can be considered the adsorption sites for effective adsorption of ethanol. In the Co-doped ZnO gas sensor, the amount of oxygen vacancies significantly decreases, according to the *p*-type behavior and leads to the observed decrease of the sensor's response.

An acid-base change related to the introduction of the Co₃O₄ phase should be considered in this case. Acid-base characteristics of the sensing material are well known for addressing the sensing performances in metal oxide semiconductor gas sensors. In the framework of this hypothesis, the high sensitivity to ethanol found in pristine ZnO could be related to a large number of electrons involved in the pathway of total oxidation of ethanol (see Equation (3) below). This is a process favored on basic sites, which are known to be relatively abundant on the ZnO surface.



In the presence of Co, the response to ethanol is lower. This can be attributed to the higher surface acidity of the Co-doped ZnO, which favors alternative pathways, e.g., through Equation (1), involving a strongly reduced number of electrons.

3.3. Hydrogen Sensor Performances

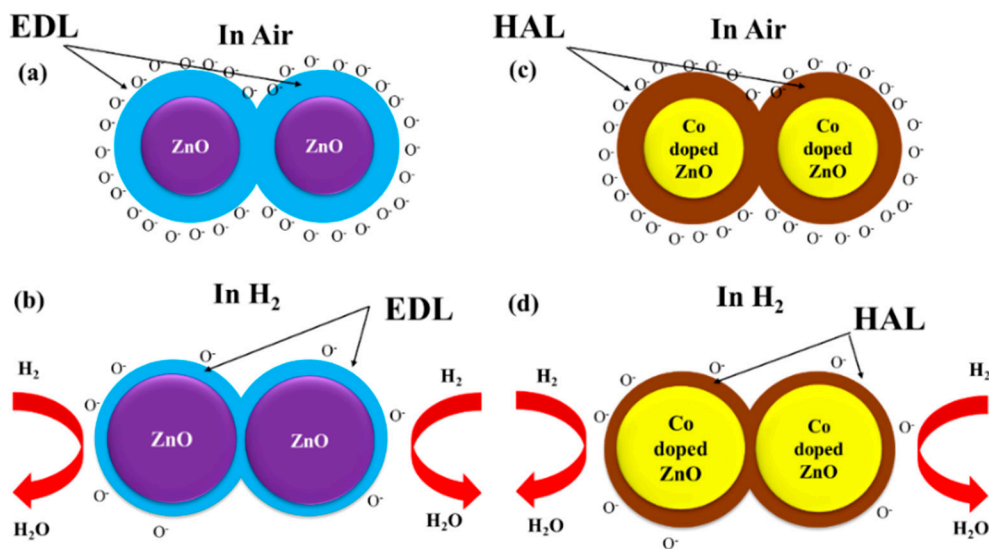
In view of the above findings, we decided to investigate the performances of the Co-doped ZnO gas sensor for hydrogen sensing at a low concentration. When the sensor is in an H₂ atmosphere, hydrogen molecules react with adsorbed oxygen ions on the surface of the gas sensor, according to the following equation [33].



The released electrons will cause modulation of electrical resistance in the gas sensor and a signal will appear, which relies on the balance between the adsorption and desorption rate of H₂ and surface reactivity with adsorbed oxygen species [1]. When the *n*-type ZnO sensor is in the air, oxygen molecules adsorb onto the sensing layer surface and, depending on the temperature, will be converted to oxygen ions (e.g., O₂⁻, O⁻ or O₂) by extraction of free electrons from the conductance band of ZnO. Adsorbed oxygen ions will generate a region free of electrons, which is known as the electron depletion layer, EDL (see Scheme 1a). In hydrogen, these molecules will be chemisorbed on the surfaces of ZnO NPs. By a subsequent reaction between the hydrogen molecules and the adsorbed oxygen species, the trapped electrons are released back to the ZnO NPs and H₂O vapor is released. Accordingly, the thickness of EDL will decrease (Scheme 1b) and the resistance of the sensor decreases.

In the case of cobalt doped ZnO gas sensors, the *p*-type semiconducting behavior was observed. As shown in Scheme 1c, after exposure to air, oxygen molecules can be adsorbed on the surface of the sensor and a hole accumulation layer (HAL) will be formed on the surface of the sensor. Upon exposure to hydrogen vapor, electrons come back to the surface of the sensor, which results in a decrease of width of HAL and an increase of the sensor's resistance (Scheme 1d). A lower response of the Co-doped ZnO sensor relative to the pristine ZnO gas sensor can be attributed to the intrinsic lower response of the *p*-type semiconductor metal oxides relative to that of *n*-type counterparts [34].

Preliminary, it was found that the optimum operating temperature determined by exposure to 50 ppm H₂ at different operating temperatures (100–375 °C) is 150 °C, which is lower than the temperature observed in a pristine ZnO sensor. In Figure 6a, one can observe that the response trend increases with a rising operating temperature. It reaches its maximum at 150 °C and then decreases gradually.



Scheme 1. Schematization of the H₂ sensing mechanism in pristine and Co-doped ZnO gas sensors.

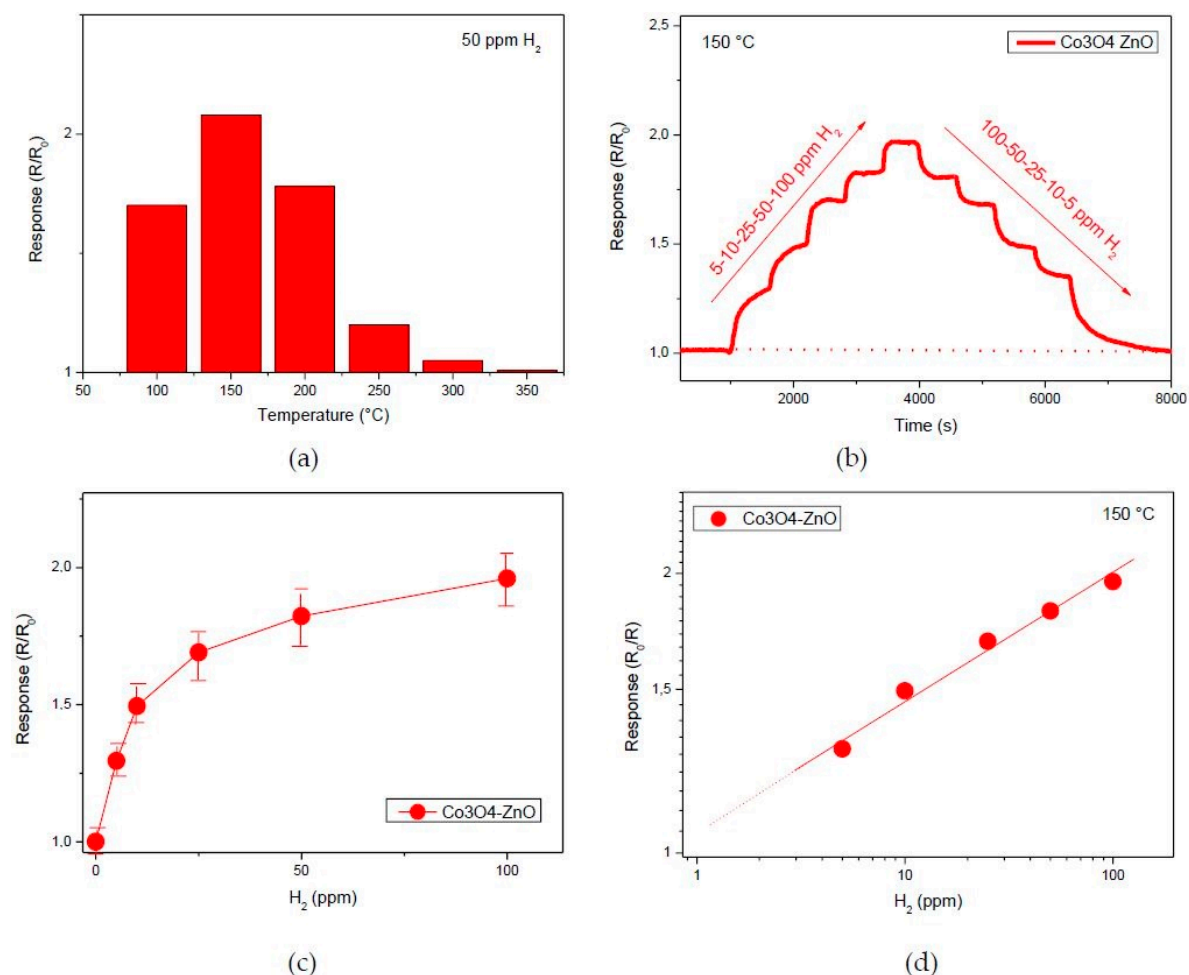


Figure 6. (a) Response vs. H₂ concentration of the Co-doped ZnO sensor recorded at different temperatures. (b) Response to increasing and decreasing H₂ concentration values at the temperature of 150 $^{\circ}\text{C}$. (c) Calibration curve in a linear scale. (d) Calibration curve in a log-log scale.

Afterward, responses of the sensor to low concentrations of H₂ were investigated at the optimum operating temperature of 150 $^{\circ}\text{C}$. The sensor has been exposed to 5, 10, 25, 50, and 100 ppm of H₂.

The exposing steps were repeated in the reverse order to verify the presence of “hysteresis” effects and the repeatability of the responses. Figure 6b depicted the results obtained, highlighting that little or no hysteresis effects are retained. The response values obtained for increasing H₂ concentrations are almost the same ones obtained when the H₂ concentrations decrease, which suggests that the gas sensing process is reproducible and the device has a good repeatability.

The calibration curve in linear scale is shown in Figure 6c. The response curve increases rapidly with the increase of the H₂ concentration below 25 ppm. However, the response growth becomes slower when the H₂ concentration is above that value, which indicates that the sensor exhibits excellent sensing performance for a low concentration of H₂. For H₂ concentrations higher than 25 ppm, the current reaches saturation during the gas exposure. The log-log scale (see Figure 6d) allows us to appreciate that the limit of detection (LOD) for hydrogen of the Co-doped ZnO sensor is effectively very low at around 1 ppm.

4. Conclusions

In summary, pristine and Co-doped ZnO NPs were synthesized via the sol-gel method for electrical and gas sensing studies. The synthesized NPs were characterized by XRD and TEM. Electrical resistance measurements showed that the pristine ZnO sensor displayed a high response to hydrogen at a low concentration in air but with poor selectivity. Co-doping in ZnO reduced the response to hydrogen. However, we noted that the selectivity increased. This effect has been attributed to the changes of some chemical and physical parameters such as the acid-base characteristics, the *p*-type behavior, and the decrease of oxygen vacancies occurring in the Co-doped ZnO sensing layer. These peculiar characteristics were allowed to realize a high performance breath hydrogen sensor based on the synthesized Co-ZnO nanocomposite, which displays a limit of detection at around 1 ppm and good selectivity for H₂ in human breath.

Author Contributions: M.E.B. and G.N. conceived the project and defined experimental protocol. F.M., R.K. and S.G.L. carried out experiments. G.N. and A.M. completed the draft of manuscript.

Funding: This research received no external funding.

Acknowledgments: Authors are grateful for the partial support from the Iran Nanotechnology Initiative Council.

Conflicts of Interest: The authors declare no conflicts of interest.

References

1. Neri, G. First fifty years of chemoresistive gas sensors. *Chemosensors* **2015**, *3*, 1–20. [[CrossRef](#)]
2. Dhawale, D.S.; Lokhande, C.D. Chemical route to synthesis of mesoporous ZnO thin films and their liquefied petroleum gas sensor performance. *J. Alloys. Compd.* **2011**, *509*, 10092–10097. [[CrossRef](#)]
3. Qi, Q.; Zeng, T.; Zeng, Y.; Yang, H. Humidity sensing properties of KCl-doped Cu-Zn/CuO-ZnO nanoparticles. *Sens. Actuators B Chem.* **2009**, *137*, 21–26. [[CrossRef](#)]
4. Lee, J.H.; Ko, K.H.; Park, B.O. Electrical and optical properties of ZnO transparent conducting films by the sol-gel method. *J. Cryst. Growth* **2003**, *247*, 119. [[CrossRef](#)]
5. Olson, D.C.; Piris, J.; Collins, R.T.; Shaheen, S.E.; Ginley, D.S. Hybrid photovoltaic devices of polymer and ZnO nanofiber composites. *Thin Solid Films* **2006**, *496*, 26. [[CrossRef](#)]
6. Powell, D.A.; Kalantar-zade, K.; Wlodarski, W. Numerical calculation of SAW sensitivity: Application to ZnO/LiTaO₃ transducers. *Sens. Actuators A Phys.* **2004**, *115*, 456–461. [[CrossRef](#)]
7. Hu, Z.J.Y.; Xu, C.; Mei, T.; Guo, J.; White, T. Monodisperse ZnO nanodots: Synthesis, characterization, and optoelectronic properties. *J. Phys. Chem. C* **2007**, *111*, 9757–9760. [[CrossRef](#)]
8. Chen, Y.L.H.; Xie, C.; Wu, J.; Zeng, D.; Liao, Y. A comparative study on UV light activated porous TiO₂ and ZnO film sensors for gas sensing at room temperature. *Ceram. Int.* **2012**, *38*, 503–509. [[CrossRef](#)]
9. Mirzaei, A.; Park, S.; Kheel, H.; Sun, G.-J.; Lee, S.; Lee, C. ZnO-capped nanorod gas sensors. *Ceram. Int.* **2016**, *42*, 6187–6197. [[CrossRef](#)]

10. Kwon, Y.J.; Kang, S.Y.; Mirzaei, A.; Choi, M.S.; Bang, J.H.; Kim, S.S.; Kim, H.W. Enhancement of gas sensing properties by the functionalization of ZnO-branched SnO₂ nanowires with Cr₂O₃ nanoparticles. *Sens. Actuators B Chem.* **2017**, *249*, 656–666. [[CrossRef](#)]
11. Mirzaei, A.; Leonardi, S.G.; Neri, G. Detection of hazardous volatile organic compounds (VOCs) by metal oxide nanostructures-based gas sensors: A review. *Ceram. Int.* **2016**, *42*, 15119–15141. [[CrossRef](#)]
12. Mirzaei, A.; Kim, J.-H.; Kim, H.W.; Kim, S.S. How shell thickness can affect the gas sensing properties of nanostructured materials: Survey of literature. *Sens. Actuators B Chem.* **2018**, *258*, 270–294. [[CrossRef](#)]
13. Leonardi, S.G. Two-dimensional zinc oxide nanostructures for gas sensor applications. *Chemosensors* **2017**, *5*, 17. [[CrossRef](#)]
14. Chu, X.; Chen, T.; Zhang, W.; Zheng, B.; Shui, H. Investigation on formaldehyde gas sensor with ZnO thick film prepared through microwave heating method. *Sens. Actuators B Chem.* **2009**, *142*, 49–54. [[CrossRef](#)]
15. Zeng, Y.; Zhang, T.; Yuan, M.; Kang, M.; Lu, G.; Wang, R.; Fan, H.; He, Y.; Yang, H. Growth and selective acetone detection based on ZnO nanorod arrays. *Sens. Actuators B Chem.* **2009**, *143*, 93–98. [[CrossRef](#)]
16. Dong, L.F.; Cui, Z.L.; Zhang, Z.K. Gas sensing properties of nano-ZnO prepared by arc plasma method. *Nanostruct. Mater.* **1997**, *8*, 815–823. [[CrossRef](#)]
17. Oh, E.; Choi, H.Y.; Jung, S.H.; Cho, S.; Kim, J.C.; Lee, K.H.; Kang, S.W.; Kim, J.; Yund, J.Y.; Jeong, S.H. High-performance NO₂ gas sensor based on ZnO nanorod grown by ultrasonic irradiation. *Sens. Actuators B Chem.* **2009**, *141*, 239–243. [[CrossRef](#)]
18. Wang, X.; Zhang, J.; Zhu, Z.; Zhu, J. Effect of Pd²⁺ doping on ZnO nanotetrapods ammonia sensor. *Colloids Surf. A* **2006**, *276*, 59–64. [[CrossRef](#)]
19. Aygün, S.; Cann, D. Hydrogen sensitivity of doped CuO/ZnO heterocontact sensors. *Sens. Actuators B Chem.* **2005**, *106*, 837–842.
20. Wei, A.; Pan, L.; Huang, W. Recent Progress in the ZnO Nanostructure-Based Sensors. *Mater. Sci. Eng. B* **2011**, *176*, 1409–1421. [[CrossRef](#)]
21. Rout, C.S.; Raju, A.R.; Govindaraj, A.; Rao, C.N.R. Hydrogen sensors based on ZnO nanoparticles. *Solid State Commun.* **2006**, *138*, 136–138. [[CrossRef](#)]
22. Hoppe, M.; Lupan, O.; Postica, V.; Wolff, N.; Duppel, V.; Kienle, L.; Tiginyanu, I.; Adelung, R. ZnAl₂O₄-Functionalized zinc oxide microstructures for highly selective hydrogen gas sensing applications. *Phys. Stat. Solidi* **2018**, *215*, 1700772.
23. Sett, D.; Basak, D. Highly enhanced H₂ gas sensing characteristics of Co: ZnO nanorods and its mechanism. *Sens. Actuators B Chem.* **2018**, *243*, 475–483. [[CrossRef](#)]
24. Reddy, P.; Reddy, K.S.; Reddy, B.; Manasa, M.V.; Devi, G.S.; Rao, G.N. Gas Sensing Characteristics of ZnO: Nb₂O₅ nanocomposite towards hydrogen gas. *J. Adv. Phys.* **2017**, *6*, 418–421. [[CrossRef](#)]
25. Jaaniso, R.; Kiang Tan, O. *Semiconductor Gas Sensors*; Woodhead Publishing Group: Sawston, UK, 2013.
26. Wang, H.T.; Kang, B.S.; Ren, F.; Tien, L.C.; Sadik, P.W.; Norton, D.P.; Pearton, S.J. Hydrogen-selective sensing at room temperature with ZnO nanorods. *J. Appl. Phys. Lett.* **2005**, *86*, 243503. [[CrossRef](#)]
27. Bekermann, D.; Gasparotto, A.; Barreca, D.; Maccato, C.; Comini, E.; Sada, C.; Sberveglieri, G.; Devi, A.; Fischer, R.A. Co₃O₄/ZnO nanocomposites: From plasma synthesis to gas sensing applications. *ACS Appl. Mater. Interfaces* **2012**, *4*, 928–934. [[CrossRef](#)]
28. Shin, W.; Goto, T.; Nagai, D.; Itoh, T.; Tsuruta, A.; Akamatsu, T.; Sato, K. Thermoelectric array sensors with selective combustion catalysts for breath gas monitoring. *Sensors* **2018**, *18*, 1579. [[CrossRef](#)]
29. Mirzaei, A.; Janghorban, K.; Hashemi, B.; Bonyani, M.; Leonardi, S.G.; Neri, G. Highly stable and selective ethanol sensor based on α -Fe₂O₃ nanoparticles prepared by Pechini sol-gel method. *Ceram. Int.* **2016**, *42*, 6136–6144. [[CrossRef](#)]
30. Anderson, P.; Baumberg, B. *Alcohol in Europe, A Public Health Perspective*; A Report for the European Commission; European Commission: Brussels, Belgium, 2006.
31. Karmaoui, M.; Leonardi, S.G.; Latino, M.; Tobaldi, D.M.; Donato, N.; Pullar, R.C.; Neri, G. Pt-decorated In₂O₃ nanoparticles and their ability as a highly sensitive (< 10 ppb) acetone sensor for biomedical applications. *Sens. Actuators B Chem.* **2016**, *230*, 697–705. [[CrossRef](#)]
32. Ghosh, A.; Bannerjee, R.; Basu Majumder, S. Selective hydrogen sensing by cobalt doped ZnO thin films: A study on carrier reversal conductivity. In Proceedings of the IEEE Sensors, Busan, South Korea, 1–4 November 2015.

33. Falsafi, F.; Hashemi, B.; Mirzaei, A.; Fazio, E.; Neri, F.; Donato, N.; Leonardi, S.G.; Neri, G. Sm-doped cobalt ferrite nanoparticles: A novel sensing material for conductometric hydrogen leak sensor. *Ceram. Int.* **2017**, *43*, 1029–1037. [[CrossRef](#)]
34. Kim, J.-H.; Lee, J.-H.; Mirzaei, A.; Kim, H.W.; Kim, S.S. Optimization and gas sensing mechanism of n-SnO₂-p-Co₃O₄ composite nanofibers. *Sens. Actuators B Chem.* **2017**, *248*, 500–511. [[CrossRef](#)]



© 2018 by the authors. Licensee MDPI, Basel, Switzerland. This article is an open access article distributed under the terms and conditions of the Creative Commons Attribution (CC BY) license (<http://creativecommons.org/licenses/by/4.0/>).